NanoNEXT

Research Article

DOI: 10.54392/nnxt2621

Aluminium-Doped Pbs Thin Films Deposited by Nebulizer Spray Pyrolysis: Structural, Optical, and Photovoltaic Properties

M. Rigana Begam [a,*], S. Elavarasan [a], A.M.S. Arulanantham [b]

[a] Department of Physics, Vel Tech Rangarajan Dr. Sagunthala R&D Institute of Science and Technology, Avadi, Chennai, Tamil Nadu 600 062, India

[b] Department of Physics, Mohamed Sathak A J College of Engineering, Chennai, Tamil Nadu 603 103, India

* Corresponding author Email: riganabegam.m@gmail.com

DOI: https://doi.org/10.54392/nnxt2621

Received: 08-01-2026; Revised: 23-03-2026; Accepted: 28-03-2026; Published: 10-04-2026

Abstract: Aluminium-doped lead sulfide (PbS) thin films were deposited on glass substrates by using a low-cost nebulizer spray pyrolysis (NSP) method for photovoltaic applications. The Aluminium content was varied from Pure to 5 Wt.% to study its effect on structural, surface, optical, and electrical properties. X-ray diffraction results confirm the formation of polycrystalline PbS with a cubic crystal structure. The films show a strong preferential orientation along the (200) plane. The crystallite size ranges between 18 and 20 nm and changes slightly with doping level. Optical studies show a clear increase in direct band gap from 1.54 eV for the Pure PbS film to 1.66 eV for the 5 Wt.% Al-doped PbS film. This shift indicates a modification in electronic structure and defect states resulting from Aluminium incorporation. Electrical analysis shows lower resistivity and higher carrier concentration at 2.5 Wt.% Al doping. The results indicate that controlled Al doping improves the optoelectronic behaviour of PbS thin films and makes them suitable for low-cost solar cell applications.

Keywords: PbS Thin Films, Aluminium Doping, Nebulizer Spray Pyrolysis, Band Gap Tuning, Photovoltaics Semiconductor Thin Films.

1. Introduction

Lead sulfide (PbS) is a well-known IV–VI semiconductor. It continues to attract strong research interest because of its narrow direct band gap, high absorption coefficient, and flexible optoelectronic properties [1]. In bulk form, PbS has a direct band gap of about 0.41 eV at room temperature. When the material is prepared as a thin film or in nanostructured form, the band gap increases due to quantum confinement. This effect arises from its large exciton Bohr radius of nearly 18 nm. Because of these features, PbS is suitable for infrared detectors, photoconductors, and solar absorber layers [2]. The material absorbs strongly in the visible and near-infrared regions. Hence, even a thin layer can absorb a large fraction of incident light, which is important for low-cost solar cells. There is renewed interest in narrow-bandgap semiconductors for advanced photovoltaic systems. Such materials are useful in tandem and hybrid solar cell designs. A semiconductor with a tunable band gap and a controlled carrier density offers great flexibility in device design and energy band alignment [3, 4]. PbS has attracted attention in both thin-film and quantum dot solar cells because its electronic structure can be tuned, and it can be processed from solution [5]. However, it remains difficult to achieve strong optical absorption together with good electrical transport. The intrinsic carrier density and defect states in PbS affect recombination, mobility, and junction properties. Therefore, controlled doping is an important approach to improve its performance [6].

Doping is a common method to modify semiconductor properties. The introduction of dopant ions changes conductivity, defect density, and band structure. Aliovalent dopants can distort the lattice, influence grain boundaries, and change the number of free carriers. These changes affect both optical and electrical behaviour. In PbS, trivalent ions such as Al^{3+} can replace Pb^{2+} ions in the lattice. This substitution can create donor-like centres and shift the Fermi level towards the conduction band. As a result, the band gap may widen due to the Burstein–Moss effect, and trap-assisted recombination may decrease. Such effects are useful for solar cell performance [7]. At the same time, excessive doping can create interstitial defects and lattice strain. These defects can scatter carriers and reduce mobility. Hence, it is necessary to study the relation between structure and electrical properties in doped PbS films. The deposition technique also plays an important role in deciding film quality. Methods such as thermal evaporation, sputtering, chemical bath deposition, and spray pyrolysis have been used to

prepare PbS films. Among these, spray pyrolysis is simple, economical, and suitable for large-area coating under atmospheric conditions. The method allows good control over precursor concentration and dopant level. It does not require complex vacuum systems. Spray techniques are also compatible with roll-to-roll processing, which supports large-scale solar module production [8]. The nebulizer spray pyrolysis (NSP) method produces fine droplets. This feature improves film uniformity and surface coverage.

Several studies have reported doped PbS thin films prepared by chemical methods. However, detailed studies on Aluminium doping using nebulizer spray pyrolysis and its effect on photovoltaic behaviour are still limited [9, 10]. Many reports focus only on structural or optical changes. Few studies connect these changes clearly with charge transport and device performance. A systematic study that links crystallinity, lattice strain, band gap tuning, carrier concentration, and photoresponse is still required. In this background, the present study reports the preparation of Al-doped PbS thin films by nebulizer spray pyrolysis. The work examines structural, morphological, optical, and electrical properties in a systematic manner. Special focus is given to the effect of Aluminium concentration on band gap and carrier transport. A simple FTO/PbS:Al photovoltaic device is also fabricated to check practical performance. This combined material and device study aims to clarify how Aluminium doping modifies PbS thin films and to evaluate their potential as low-cost absorber layers for future photovoltaic applications.

2. Experimental Procedure

2.1 Thin Film Deposition

Aluminium-doped lead sulfide (PbS:Al) thin films were deposited on optically polished glass substrates by the Nebulizer Spray Pyrolysis (NSP) method. Spray pyrolysis is a simple and low-cost technique for preparing semiconductor films. It is suitable for large-area coating and works under atmospheric conditions. The method allows good control over composition and dopant level through solution chemistry. It does not require a vacuum system, which makes it practical for scalable production. The glass substrates were cleaned carefully before deposition. First, the substrates were washed with laboratory detergent and rinsed with double-distilled water. Then, they were treated with a dilute acid solution to remove inorganic impurities. After that, ultrasonic cleaning was carried out in acetone and ethanol to remove organic residues. Finally, the substrates were dried using hot air. Clean surface condition is important in spray deposition because film growth depends on surface energy and wettability. Any contamination can disturb nucleation and reduce film quality.

Analytical grade lead nitrate ($Pb(NO_3)_2$) was used as the lead source, and thiourea (CH_4N_2S) was used as the sulfur source. Thiourea releases sulfide ions in a controlled way during thermal decomposition, which supports uniform PbS formation. Aluminium chloride ($AlCl_3$) was selected as the dopant source because it dissolves easily in water and provides Al^{3+} ions for lattice incorporation. Lead nitrate and thiourea were dissolved separately in deionized water in a 1:1 molar ratio. The two solutions were mixed and stirred continuously to obtain a homogeneous precursor solution. Aluminium chloride was added in suitable amounts to achieve doping levels of Pure PbS, 2.5 Wt.%, and 5 Wt.% with respect to lead content. The total solution volume was kept constant to maintain reproducibility. The solution was stirred for about 10–15 minutes until a clear and stable mixture was obtained.

The deposition process used a glass nebulizer connected to a compressed air supply. The nebulizer converted the precursor solution into fine aerosol droplets. The substrates were placed on a hot plate maintained at 400 °C. This temperature ensures complete thermal decomposition of the sprayed droplets and formation of crystalline PbS phase, as reported in earlier spray pyrolysis studies of chalcogenide films [11]. The carrier gas pressure and spray rate were adjusted carefully to ensure uniform coverage and to avoid excessive wetting of the substrate surface. When the droplets reached the heated substrate, solvent evaporation occurred first. This step was followed by solute precipitation and thermal decomposition. Lead and sulfur ions reacted to form PbS directly on the substrate surface. Aluminium ions were incorporated into the lattice either by replacing Pb^{2+} ions or by occupying interstitial sites, depending on concentration. The entire deposition process was carried out in a partially closed chamber to remove gaseous by-products safely. The schematic diagram of the setup is shown in Figure 1. After deposition, the films cooled naturally to room temperature. Slow cooling helped to reduce thermal stress and avoid cracks. The deposited films showed a uniform greyish-black colour, which is typical for PbS thin films.

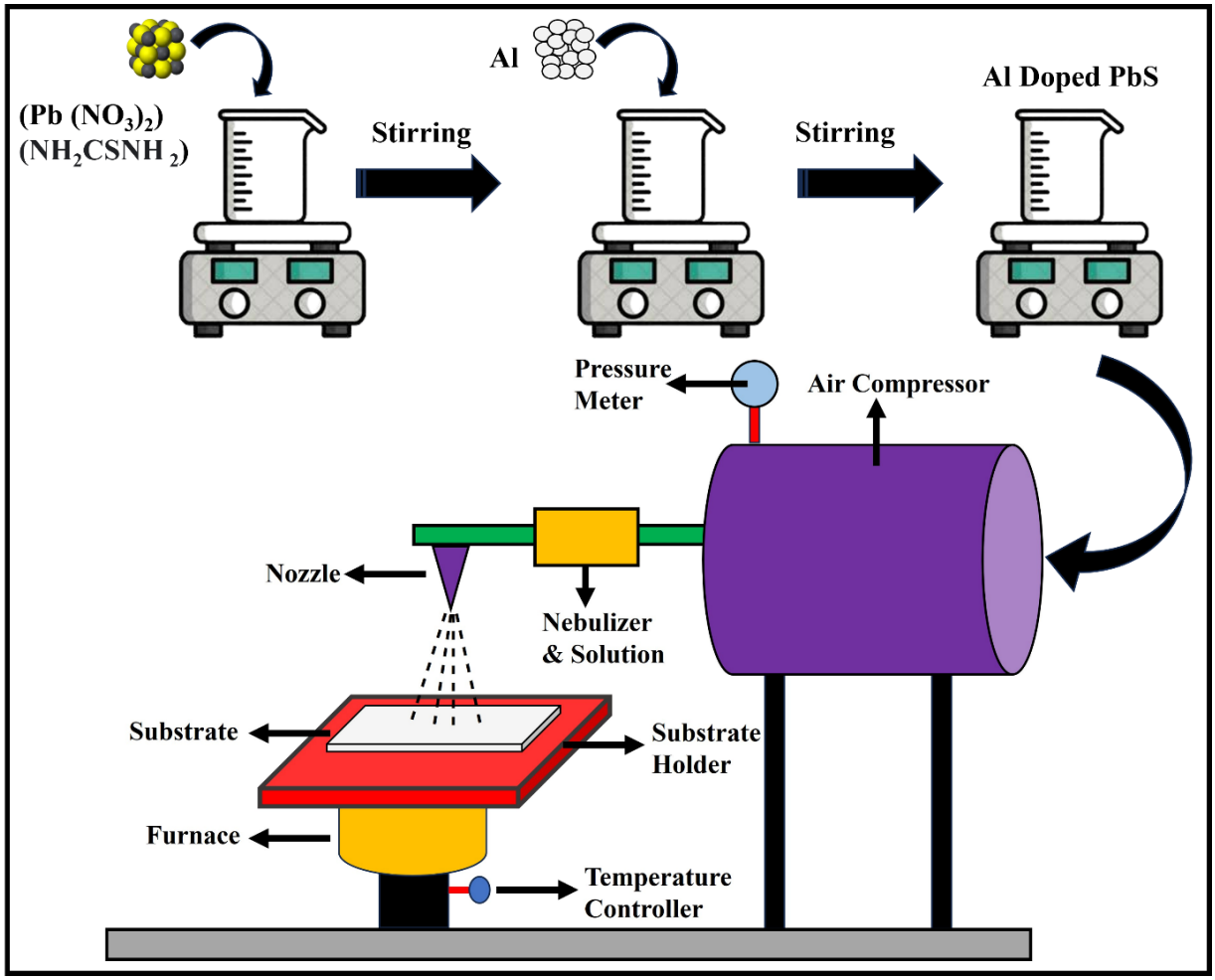

Figure 1. Schematic Illustration of the Preparation of Pure and Al-Doped PbS Thin Films by Nebulizer Spray Pyrolysis Technique.

2.2 Characterization Techniques

The structural properties of the films were studied using X-ray diffraction (XRD) with a Bruker D8 Advance diffractometer using CuKα radiation (λ = 1.5418 Å). Diffraction patterns were recorded in the 2θ range of 10°–80°. XRD confirms phase formation, crystal structure, and lattice changes due to doping. Crystallite size was estimated using the Scherrer equation, which is widely used for nanocrystalline semiconductor films [12]. Surface morphology was examined using a field-emission scanning electron microscope (FEI Quanta FEG 200). The microstructure and grain distribution were analysed from SEM images. Elemental composition was confirmed using energy-dispersive X-ray spectroscopy (EDS) attached to the SEM system. Grain size and connectivity are important for photovoltaic films because grain boundaries can act as recombination centres and influence carrier movement. Optical properties were measured using a double beam UV–Vis–NIR spectrophotometer (Jasco V-670). Transmittance data were recorded in the visible and near-infrared region. The absorption coefficient was calculated from transmittance values. The optical band gap was determined using Tauc's relation for direct-band-gap semiconductors. This method is commonly used for chalcogenide thin films [13]. Electrical conductivity and current–voltage (I–V) characteristics were measured using a Keithley 2450 source meter. These characterization methods helped to establish a clear link between Aluminium doping, structural changes, optical band-gap variation, and electrical behaviour in PbS thin films.

3. Results and Discussion

3.1 XRD Analysis

The crystal structure and phase purity of the Pure PbS and Al-doped PbS thin films were studied using X-ray diffraction. The diffraction patterns were recorded in the 2θ range of 10°–80°. The patterns confirm the formation of polycrystalline PbS with a cubic rock-salt structure, as shown in Figure 2. The main diffraction peaks correspond to the (100), (200), (220), and (311) planes. These peaks match well with the standard

JCPDS data (00-001-0880) for cubic PbS. No extra peaks related to Aluminium compounds are observed. This result shows that Aluminium ions entered the PbS lattice without forming secondary phases. Similar structural stability under controlled doping has been reported earlier for chalcogenide thin films [14]. All films show a strong orientation along the (200) plane. This preferred growth direction is common in spray-deposited PbS films. The growth process depends on surface energy and thermal conditions during deposition. The sharp diffraction peaks indicate good crystallinity. When the Aluminium concentration increases from Pure PbS to 5 Wt.%, the peak intensity decreases slightly, and the peaks become broader. Peak broadening suggests a reduction in crystallite size and an increase in lattice strain due to dopant incorporation.

$$D = K\lambda \,/\, \beta cos\theta$$

The average crystallite size was calculated using the Scherrer equation,

where λ is the X-ray wavelength (1.5418 Å), β is the full width at half maximum, and θ is the Bragg angle. The crystallite size decreases from 19.67 nm for Pure PbS to 18.82 nm at 2.5 Wt.% Al-doped PbS. This decrease indicates that moderate Aluminium addition disturbs the lattice and limits grain growth. At 5 Wt.% doping, the crystallite size increases slightly to 20.05 nm. This change may result from partial strain relaxation or dopant clustering at higher concentrations. Microstrain and dislocation density were also calculated to understand defect formation. Microstrain was estimated using the relation

$$\varepsilon = \beta cos\theta \,/\, 4$$

And the dislocation density was calculated from

$$\delta = 1/D2$$

The microstrain increases from 0.397×10^{-3} for the undoped film to 0.478×10^{-3} at 2.5 Wt.% Al. This increase confirms that Aluminium ions create local lattice distortion. The ionic radius of Al^{3+} is smaller than that of Pb^{2+}. When Al^{3+} replaces Pb^{2+} in the lattice, compressive strain develops. Similar strain effects in doped PbS films have been reported earlier and are known to influence electronic structure and carrier transport [8].

The dislocation density shows a similar trend. It increases at 2.5 Wt.% doping and decreases slightly at 5 Wt.%. A higher dislocation density indicates more structural defects (Table 1). These defects can scatter charge carriers and reduce mobility. However, a controlled number of defects can help in tuning electronic properties. In photovoltaic materials, defect chemistry plays an important role in recombination behaviour. The lattice constant increases gradually with Aluminium concentration. This increase suggests lattice distortion due to dopant incorporation. Although Aluminium has a smaller ionic radius, lattice expansion may occur due to defect complexes or sulfur vacancy formation. Earlier studies on doped PbS systems have also reported similar variation in lattice parameters due to charge compensation effects. The XRD results confirm that Aluminium doping modifies microstructural parameters without changing the cubic phase of PbS. Moderate doping reduces crystallite size and increases strain and defect density. These changes indicate successful incorporation of Al ions into the lattice. Such structural modifications are expected to affect the optical band gap and electrical transport, which are discussed in the following sections.

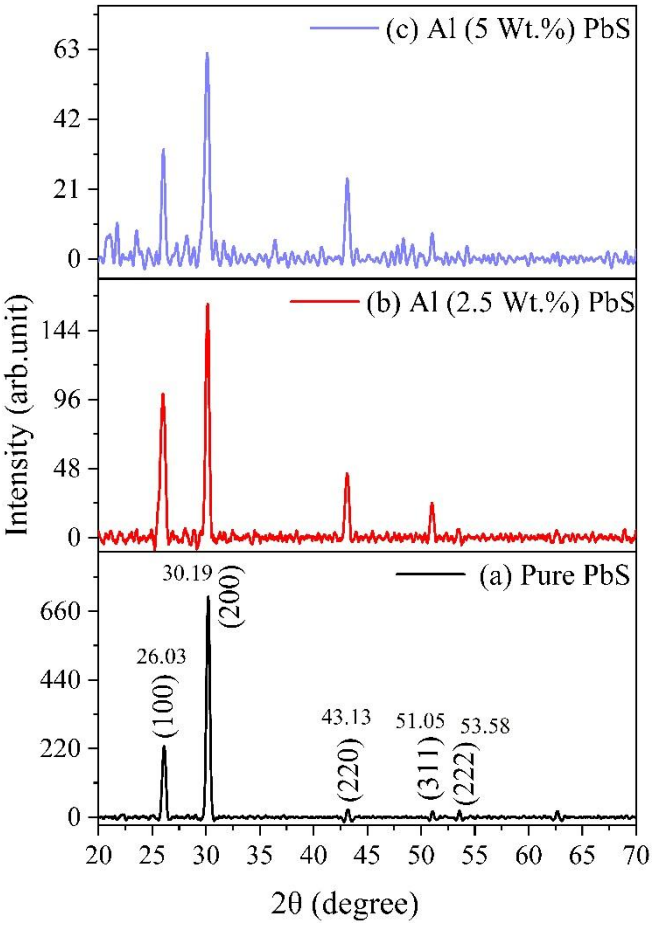

Figure 2. XRD patterns of Pure PbS and Al-doped PbS thin films.

3.2 Optical Properties

The optical properties of the Pure and Al-doped PbS thin films were studied using UV–Vis spectroscopy.

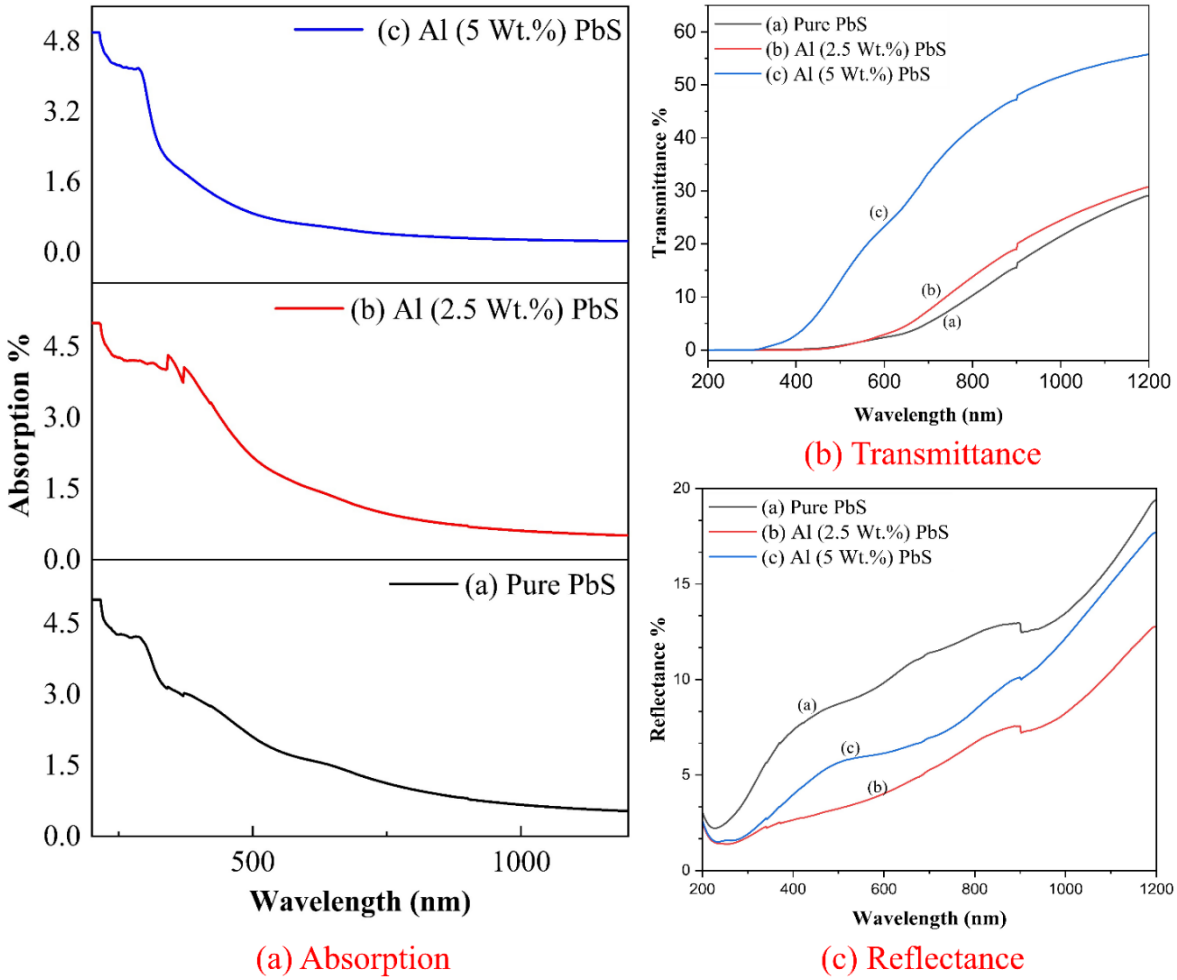

Table 1. Structural parameters and Lattice constants variation of Pure PbS and Al-doped Pbs thin films.

Samples	Crystal Size(nm)	Dislocation(δ)x 10^{-3}(nm^{-2})	Stain ε x10^{-3}	Lattice constant A
Pure PbS	19.671	2.584	0.397	5.914
Al (2.5 Wt.%) PbS	18.821	2.822	0.4786	6.421
Al (5 Wt.%) PbS	20.050	2.487	0.450	6.653

Figure 3. Optical Properties of Pure and Al-Doped PbS Thin Films: **(a)** Absorption, **(b)** Transmittance, and **(c)** Reflectance Spectra.

The measurements covered the wavelength region near the fundamental absorption edge. Figure 3 (a–c) shows the absorption, transmittance, and reflectance spectra of the prepared films. The absorption coefficient (α) was calculated from the measured transmittance data by using the standard relation between film thickness and optical transmission. PbS is a direct band gap semiconductor. It shows strong absorption in the visible and near-infrared regions. This property makes it suitable for photovoltaic and optoelectronic devices. The absorption spectra show a clear and sharp absorption edge. This feature confirms direct electronic transitions between the valence band and the conduction band. The optical band gap (Eg) was calculated using the Tauc relation for direct transitions, given by

$$(\alpha h\nu)^2 = A(h\nu - Eg)$$

where hν represents photon energy, and A is a constant. The linear portion of the $(\alpha h\nu)^2$ versus hν plot was extended to meet the energy axis. The intercept on the energy axis gives the value of the direct band gap.

The Pure PbS thin film shows a band gap of 1.54 eV. This value exceeds the bulk PbS band gap of approximately 0.41 eV. The increase is due to quantum confinement and small crystallite size in thin film form. Similar band gap widening has been reported in nanocrystalline PbS due to confinement and structural disorder. After Aluminium doping, the band gap increases gradually. It reaches 1.60 eV for 2.5 Wt.% Al and 1.66 eV for 5 Wt.% Al. The absorption edge shifts to shorter wavelengths, indicating a blue shift. This change confirms that Aluminium modifies the electronic structure of PbS. The increase in band gap can be explained mainly by the Burstein–Moss effect [15]. When carrier concentration increases, the Fermi level moves into the conduction band in n-type semiconductors. The lower energy states in the conduction band become filled. As a result, electrons require higher photon energy for transition. This process leads to an apparent increase in the optical band gap. Aluminium ions can replace Pb^{2+} ions and act as donor centres. This substitution increases free electron concentration and causes band filling.

Sulfur vacancies and lattice distortion also affect carrier generation and defect levels. The 2.5 Wt.% Al-doped film shows a good balance between higher carrier concentration and structural stability. This condition improves optical performance without large defect scattering. For 5 Wt.% Al doping, excess Aluminium may occupy interstitial sites or create more lattice disorder. These changes can influence carrier mobility and slightly alter optical transitions. The gradual increase in band gap from 1.54 eV to 1.66 eV shows that Aluminium doping is an effective method for band gap tuning in PbS thin films. Band gap control is important for solar cells because the absorber energy level must match the solar spectrum for better efficiency. The results confirm that optimized Al doping improves optical transparency and increases band gap energy. It also modifies electronic transitions in a controlled way. These features make PbS:Al thin films suitable for solar cells and optoelectronic applications [16].

3.3 EDS Analysis

The elemental composition of the films was examined using energy dispersive X-ray spectroscopy (EDS) attached to the field-emission scanning electron microscope. The representative EDS spectrum of the Al-doped PbS thin film is shown in Figure 4. The spectrum shows clear peaks corresponding to lead (Pb) and sulfur (S). These peaks confirm the formation of PbS as the main phase in the deposited films. In addition, a distinct Aluminium (Al) peak is visible. This peak confirms that Aluminium is present in the film and has been incorporated successfully into the PbS matrix. Signals related to silicon (Si) and oxygen (O) are also detected in the spectrum. These peaks arise from the glass substrate and minor surface oxidation. Such signals are common in thin films deposited on glass because the electron beam can penetrate the substrate. These signals do not indicate the formation of unwanted secondary phases in the film.

The Pb peaks appear prominently near the Pb M and Pb L energy regions, while the sulfur peak is observed near the S Kα region. The Aluminium peak appears near the Al Kα energy region around 1.49 keV. The clear detection of Aluminium without any additional impurity peaks suggests that Al ions are incorporated into the PbS lattice rather than forming separate Aluminium oxide or other compounds. Earlier reports on doped chalcogenide thin films have also shown that trivalent dopants can enter the host lattice without phase segregation. Quantitative EDS analysis shows that the Pb:S atomic ratio is close to the expected stoichiometric value. A slight sulfur deficiency is observed in some samples. This deficiency is common in spray-deposited PbS films because sulfur can evaporate during thermal decomposition at high substrate temperatures. Sulfur vacancies can act as donor-like defects and may increase carrier concentration in moderately doped films. The measured Aluminium content is close to the intended precursor concentration. This result confirms that nebulizer spray pyrolysis allows good control over film composition. The EDS results confirm the successful preparation of Al-doped PbS thin films with near-stoichiometric composition. No unwanted impurity phases are detected. The elemental distribution is uniform across the analysed region. These findings support the structural and optical results and show that Aluminium doping modifies the physicochemical properties of PbS thin films in a controlled manner for photovoltaic applications.

3.4 Morphological Analysis

The surface morphology of the Pure and Al-doped PbS thin films was studied using scanning electron microscopy. Figure 5 (a–c) shows the SEM images of the films with different Aluminium concentrations. Surface morphology plays an important role in thin-film solar cells. Grain size, grain boundaries, and surface compactness directly affect carrier movement and recombination. Hence, a morphological study is necessary to connect structural and optical

changes with device performance. The Pure PbS film shows uniform and nearly spherical nanograins. The grains cover the entire substrate surface without cracks or large voids. The film appears dense and continuous.

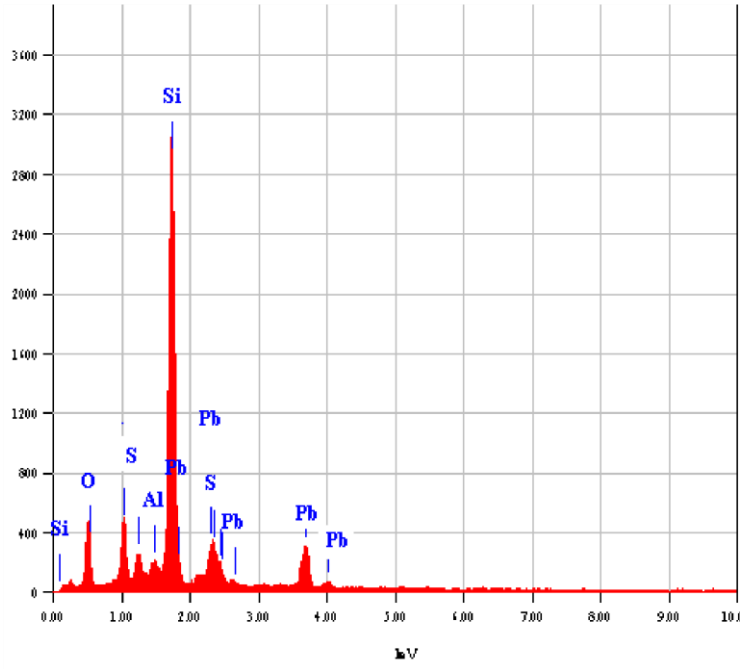

Figure 4. EDS spectrum of 2.5 Wt.% Al-doped PbS thin film.

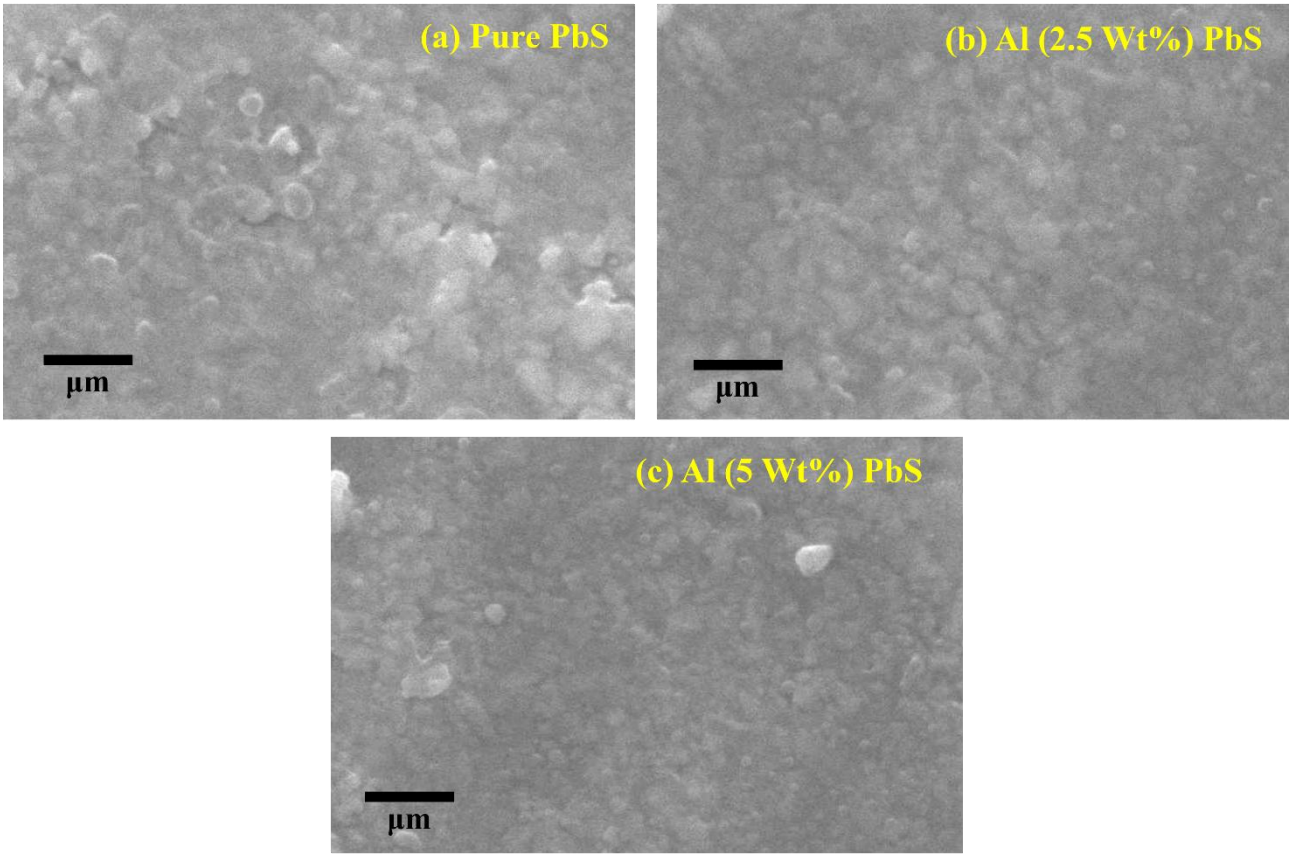

Figure 5. SEM images of Pure PbS and Al-doped PbS thin films.

This type of morphology is common in spray-deposited PbS films. Proper droplet decomposition at high substrate temperature supports uniform nucleation and grain growth. Similar spherical grains and compact surfaces have been reported for spray pyrolysed PbS films [17]. The absence of major pinholes indicates good precursor mixing and proper thermal decomposition during deposition.

After adding 2.5 Wt.% Aluminium, the surface shows slight changes. The grains maintain their spherical shape, but mild agglomeration is visible. Grain boundaries appear clearer than in the undoped film. The number of visible pinholes reduces. This change suggests that moderate Aluminium doping improves surface compactness. Aluminium ions can influence nucleation and surface diffusion during growth. Doping can change surface energy and affect how grains merge. Better grain connectivity reduces open voids and supports improved charge transport across the film. At 5 Wt.% Aluminium, the film shows a more compact and tightly packed structure. The grains appear uniform and strongly merged. The surface has very few visible pinholes. However, excessive agglomeration is also present. In some regions, grain boundaries are not clearly visible. This behaviour indicates that higher dopant concentration changes growth dynamics. Excess Aluminium may enter substitutional or interstitial positions. These changes can increase local lattice strain and modify surface diffusion. Although a compact surface reduces shunt paths in solar devices, high dopant concentration may create internal defects. These defects can affect carrier mobility, which agrees with the structural results.

The changes observed in the SEM images agree with the XRD analysis. Moderate doping reduces crystallite size and increases microstrain. These effects match the grain behaviour seen in the images. At 2.5 Wt.% Aluminium, the film shows a good balance between grain growth and defect formation. The surface remains uniform without serious structural damage. This condition supports smooth carrier transport and limits defect scattering. EDS analysis carried out along with SEM confirms the presence of Pb, S, and Al in the doped films. No extra peaks related to unwanted compounds are detected. This result confirms that Aluminium enters the PbS lattice and does not form separate oxide or chloride phases. High phase purity is important to maintain stable electronic properties and reduce recombination centres. Overall, SEM and EDS results show that Aluminium doping changes the surface morphology of PbS thin films. Moderate doping at 2.5 Wt.% improves grain connectivity and reduces surface defects. Higher doping produces a denser but more strained structure. These observations highlight the need for careful control of dopant level to achieve good structural stability and efficient electronic performance in PbS:Al thin films for solar energy applications.

3.5 Electrical and Photovoltaic Performance

The electrical transport behaviour of undoped and 5 Wt.% Al-doped PbS thin films were investigated through current–voltage (I–V) measurements in the voltage range from –5 V to +5 V. Figure 6 shows the dark and illuminated I–V characteristics of the films. The curves exhibit nearly linear and symmetric behaviour in both bias directions, indicating the formation of ohmic contacts between the electrodes and the PbS layer. Such linearity confirms that carrier transport is dominated by bulk conduction rather than interface-limited mechanisms. In the dark condition (Figure 6), the undoped PbS film exhibits relatively low current throughout the applied voltage range. At (+5 V), the current remains in the order of 10^{-8} µA, indicating higher resistivity and limited free carrier density. In contrast, the 5 Wt.% Al-doped PbS film shows a significantly enhanced current response. At +5 V, the current increases by nearly one order of magnitude compared to the undoped sample. Similarly, under reverse bias –5 V, the doped film exhibits higher absolute current values. The slope of the I–V curve becomes steeper after Aluminium incorporation, confirming reduced resistive losses and improved electrical conductivity.

The enhancement in current with Al doping can be attributed to the substitutional incorporation of Al^{3+} ions at Pb^{2+} lattice sites. This aliovalent substitution introduces additional free carriers and shifts the Fermi level towards the conduction band. The improved carrier density lowers bulk resistivity and enhances charge transport across the film. Furthermore, the structural results showed acceptable crystallinity with controlled microstrain at this doping level, which supports effective carrier mobility. Although higher doping may introduce localized defects, the present concentration maintains continuous conduction pathways without severe carrier trapping. The inset of Figure 6 shows the illuminated I–V characteristics under a light intensity of 100 W/m². Upon illumination, both films exhibit an increase in current over the entire voltage range, confirming their photoactive nature.

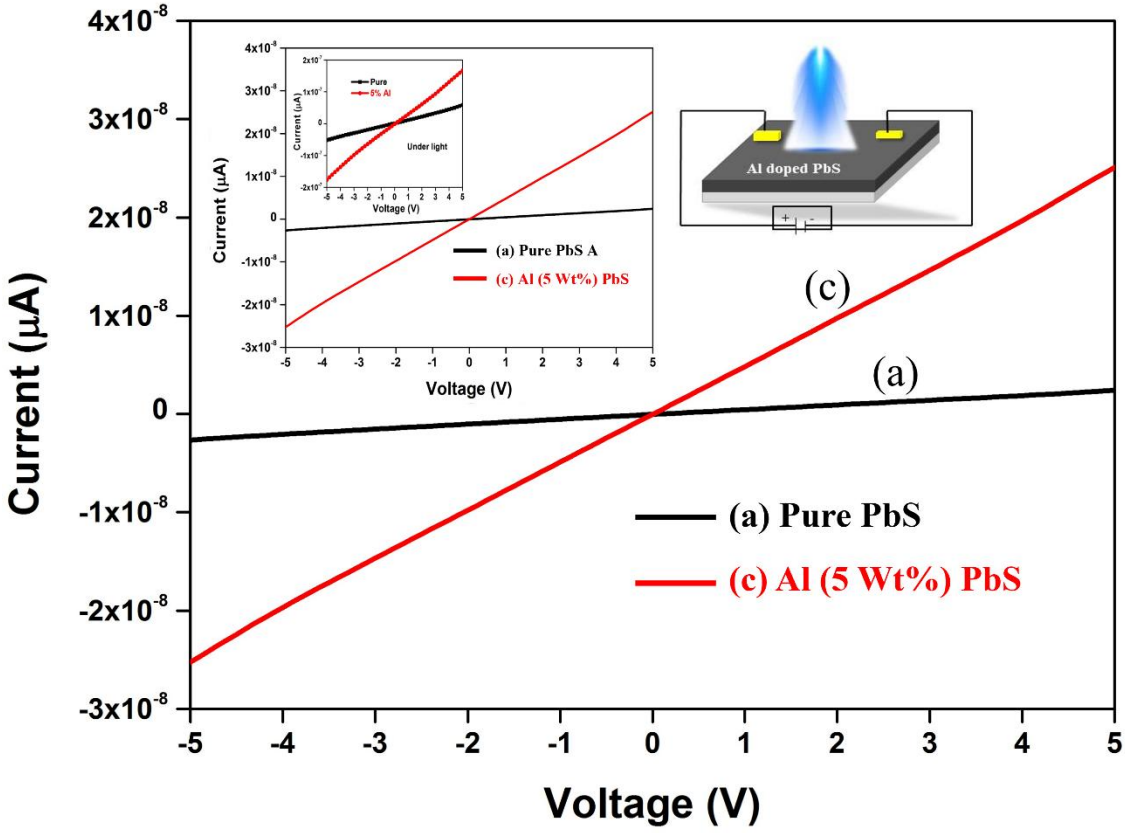

Figure 6. Current–Voltage (I-V) Response of Pure PbS and Al 5 Wt.% PbS Thin Films.

However, the magnitude of photocurrent in 5 Wt.% Al-doped film is considerably higher than that of the undoped film. The photocurrent enhancement indicates more efficient photogeneration and separation of charge carriers. Aluminium doping improves internal electric field strength and reduces recombination losses, thereby contributing to higher photocurrent.

The enhanced electrical and photoresponse characteristics of the 5 Wt.% Al-doped PbS film can be correlated with earlier structural and optical observations. Band gap widening due to the Burstein–Moss effect and improved grain compactness observed in SEM analysis support better charge carrier dynamics. The improved conductivity and higher photocurrent demonstrate that Aluminium doping effectively tailors the electronic structure of PbS thin films. Overall, the updated I–V results clearly demonstrate that Aluminium incorporation significantly improves electrical conduction and photovoltaic response. The 5 Wt.% Al-doped PbS film exhibits superior current transport and enhanced photoresponse compared to the undoped sample. These findings confirm that controlled Al doping via nebulizer spray pyrolysis is an effective strategy for improving the optoelectronic performance of PbS thin films for low-cost photovoltaic and photodetector applications.

4. Conclusion

Pure and Aluminium-doped PbS thin films were successfully prepared on glass substrates by nebulizer spray pyrolysis. This technique provides a simple and scalable method for depositing chalcogenide absorber layers at low cost. Structural analysis confirms the formation of polycrystalline cubic PbS with preferred growth along the (200) plane. Aluminium addition modifies lattice parameters, microstrain, and crystallite size. These changes indicate proper incorporation of dopant ions into the PbS lattice without forming unwanted secondary phases. Moderate Aluminium content improves structural quality and maintains phase purity. Optical studies show a steady increase in direct band gap from 1.54 eV to 1.66 eV as Aluminium concentration increases from 0 to 5 Wt.%. This variation occurs due to higher carrier concentration and band filling effect at doped levels. Structural refinement and reduced defect density at optimised doping also support this shift. Band gap tuning in this range is important for photovoltaic absorber layers because energy alignment strongly affects device performance. Electrical measurements show that Aluminium doping increases carrier concentration and decreases resistivity up to 2.5 Wt.%. Beyond this level, defect scattering affects charge transport. The film with 2.5 Wt.% Al shows better grain

connectivity, stable structure, and improved conductivity. The overall study confirms that controlled Aluminium doping tailors the structural, optical, and electrical behaviour of PbS thin films. Nebulizer spray pyrolysis proves to be an effective method for large-area deposition of doped PbS layers. This approach offers a practical route for developing advanced tunable and low-cost photovoltaic absorber materials in the future.

References

[1] T. S. Shyju, S. Anandhi, R. Sivakumar, R. Gopalakrishnan, Studies on lead sulfide (PbS) semiconducting thin films deposited from nanoparticles and its NLO application. International Journal of Nanoscience, 13(1), (2014) 1450001. https://doi.org/10.1142/S0219581X1450001X

[2] Z. Sang, C. Zhang, X. Yin, G. Qian, H. Liu, W. Que, High-performance PbS quantum dots photodetector based on NiOx/PbS-EDT heterojunction hole transport layer. Journal of Alloys and Compounds, 1036, (2025) 181671. https://doi.org/10.1016/j.jallcom.2025.181671

[3] L.-Y. Chen, T. Sun, T.J. Zhang, Y. Xie, J.M. Zhang, Modulating the band alignment, carrier mobility and optical absorption of graphene/MoS_2 heterostructure via synergistic effects of doping and strain. Surfaces and Interfaces, 46, (2024) 104024. https://doi.org/10.1016/j.surfin.2024.104024

[4] S. M. Chintapalli, L. Li, S. M. Thon, PbS colloidal quantum dot photovoltaics: progress towards infrared and flexible applications. Chemical. Communication, 61(74), (2025) 14073–14086. https://doi.org/10.1039/D5CC03198B

[5] Z. Zafar, S. Yi, J. Li, C. Li, Y. Zhu, A. Zada, W. Yao, Z. Liu, X. Yue, Recent development in defects engineered photocatalysts: an overview of the experimental and theoretical strategies. Energy Environmental Materials, 5(1), (2022) 68–114. https://doi.org/10.1002/eem2.12171

[6] X. Gao, R. Guo and B. Li, Impact of Al^{3+} incorporation on microstructural pattern, optical and electrical behaviors of PbS:Al^{3+} films from an alkaline chemical bath. Physica Scripta, 96(9), (2021) 095810. https://doi.org/10.1088/1402-4896/ac0a2b

[7] T.I. Alanazi, Current spray-coating approaches to manufacture perovskite solar cells. Results in Physics, 44, (2023) 106144. https://doi.org/10.1016/j.rinp.2022.106144

[8] S. Rex Rosario, I. Kulandaisamy, K. Deva Arun Kumar, A.M.S. Arulanantham, S. Valanarasu, M.A. Youssef, N.S. Awwad, Deposition of p-type Al doped PbS thin films for heterostructure solar cell device using feasible nebulizer spray pyrolysis technique. Physica B Condensed Matter, 575, (2019) 411704. https://doi.org/10.1016/j.physb.2019.411704

[9] S.R. Rosario, I. Kulandaisamy, A.M.S. Arulanantham, K.D.A. Kumar, S. Valanarasu, M. S. Hamdy, K. S. Al-Namshah, A. M. Alhanash, Analysis of Cu doping concentration on PbS thin films for the fabrication of solar cell using feasible nebulizer spray pyrolysis. Materials Research Express, 6(5), (2019) 056201. https://doi.org/10.1088/2053-1591/aafb9a

[10] Z. Liu, Z. Xi, L. Gu, S. Yan, R. Zhang, X. Zhang, H. Wang, J.H. Zhang, W. Tang, Energy-band engineering and deep-ultraviolet photodetection of Ga_2O_3 alloys: a concise review. Nanotechnology, 36(36), (2025) 362001. https://doi.org/10.1088/1361-6528/ae0043

[11] Q. Lv, R. Li, L. Fan, Z. Huang, Z. Huan, M. Yu, H. Li, G. Liu, G. Qiao, J. Liu, High detectivity of PbS films deposited on quartz substrates: the role of enhanced photogenerated carrier separation. Sensors, 23(20), (2023) 8413. https://doi.org/10.3390/s23208413

[12] S. Nasiri, M. Rabiei, A. Palevicius, G. Janusas, A. Vilkauskas, V. Nutalapati, A. Monshi, Modified Scherrer equation to calculate crystal size by XRD with high accuracy: examples Fe_2O_3, TiO_2 and V_2O_5. Nano Trends, 3, (2023) 100015. https://doi.org/10.1016/j.nwnano.2023.100015

[13] P. Makuła, M. Pacia and W. Macyk, How to correctly determine the band gap energy of modified semiconductor photocatalysts based on UV–Vis spectra. The Journal of Physical Chemistry Letters, 9(23), (2018) 6814–6817. https://doi.org/10.1021/acs.jpclett.8b02892

[14] N. Wichaiyo, M. Kitiwan, Q. Shen, W. Yindeesuk, The effect of PbS colloidal quantum dots with CdS and ZnS coating on photovoltaic properties. Current Applied Science and Technology, 23(2), (2022). https://doi.org/10.55003/cast.2022.02.23.011

[15] Z. Zarhri, A.D. Cano, O. Oubram, Y. Ziat, A. Bassam, Optical measurements and Burstein–Moss effect in optical properties of Nb-doped $BaSnO_3$ perovskite. Micro and Nanostructures, 166, (2022) 207223. https://doi.org/10.1016/j.micrna.2022.207223

[16] L. Lin, Y. Chen, H. Tao, L. Yao, J. Huang, L. Zhu, M. Lou, R. Chen, L. Yan, Z. Zhang, Ferromagnetism and optical properties of SnS_2 doped with two impurities: first-principles calculations. Physical. Chemistry Chemical Physics, 23(11), (2021) 6574–6582. https://doi.org/10.1039/D0CP06322C

[17] S. Ravishankar, A.R. Balu, V. S. Nagarethinam, Effect of Gd^{3+} ions on the thermal behavior, optical, electrical and magnetic properties of PbS thin films. Journal of Electronic Materials, 47(2), (2018) 1271–1278. https://doi.org/10.1007/s11664-017-5910-1

Author Contribution Statement

M. Rigana Begam: Conceptualization, Methodology, Writing - Original Draft, Investigation, Validation. S. Elavarasan: Methodology, Writing - Original Draft. A.M.S. Arulanantham: Data curation, Writing - Review & Editing. All the authors read and approved the final version of the manuscript.

Does this article screened for similarity?

Yes

Data Availability Statement

Data will be a made available on request from corresponding author non reasonable request.

Conflict of interest

The Author's declares that there is no conflict of interest anywhere.

About the License